doi.org/10.36721/PJPS.2023.36.6.REG.1793-1801.1

# Preparation of Lamivudinyl palmitate nanoemulsome for liver-targeting delivery

**Chang Liu, Tao Xu, Xiaoyu Sui, jing Wang, Cuiyan Han, Xiaoxing Ma, Jiayi Qian and Wenquan Zhu***
College of Pharmacy, Qiqihar Medical University, Qiqihar, China

**Abstract**: The water solubility and side effects of lamivudine limit its application for the treatment of viral hepatitis type B and human immunodeficiency virus. In order to increase the solubility of LA and improve the in vivo membrane permeability of the drug, LA was modified with hexadecane acid to prepare the prodrug lamivudine palmitic acid (LAP) and loaded into nanoemulsome (NES). LAP-NES was prepared by the thin film dispersion method. The LAP-NES showed the sustained release performance up to 72h in pH 7.4 PBS. Moreover, the pharmacokinetics of LAP-NES after tail vein injection in rats and the biodistribution characteristics were evaluated. The tmax of LAP-NES was 2.5h. The t1/2, clearance rate and average retention time of LAP-NES obviously prolonged compared with free LAP. The tissue biodistribution behavior of NES in vivo showed the good targeting in the liver and spleen, with the maximum at 4h and then the fluorescence slowly decreased until 72h. LAP-NES could significantly delay the release of LA in vivo, effectively prolong the elimination time, and had obvious liver-targeting ability. In summary, LAP-NES shows great potential for liver-targeting delivery to increase the therapeutic effect and decrease the side effects of LA.

**Keywords**: Lamivudine, lamivudine palmitate, nanoemulsome, liver-targeting, *in vivo* biodistribution.

## INTRODUCTION

Chronic hepatitis B is an infectious disease caused by the hepatitis B virus, which has been added to the list of Class 1 carcinogens in 2017, and has attracted the attention of the World Health Organization (Belopolskaya *et al*., 2021). Clearing hepatitis B virus is the key to the treatment of chronic hepatitis B. However, drugs used to inhibit hepatitis B virus in clinical practice have certain toxic side effects, and one of the main reasons for this problem is that the drugs are easy to spread in the body, have relatively average tissue distribution, and fail to form higher concentrations in the liver. Lamivudine (LA), known as 2', 3'-dideoxy3-thiocytosine (3TC), is the first nucleoside analogue approved for treating the infection from chronic hepatitis B virus (Martinez de Lagran *et al*., 2022, Stinco *et al*., 2021, Chow *et al*., 2023). Clinically, it is mainly used for the treatment of chronic hepatitis B, liver cirrhosis after hepatitis B, HIV infection and the combination of HBV and HIV infection. Lamivudine is a nucleoside antiviral drug developed by Biochem Pharma in Canada and first marketed in the United States by Glaxo Wellcome in the UK in 1995. It is mainly used for the treatment of chronic hepatitis B (Guo *et al*., 2020).

It has been reported that taking LA for more than 3 years can reduce the incidence of liver cancer by 51% and liver cirrhosis by 55%. Since hepatitis B virus cannot be completely cured, the insufficient therapeutic effect of 3TC is urgently needed to be enhanced in long-term medication (Choi, *et al*., 2020). In addition to long-term drug resistance problems resulting in decreased treatment effectiveness, the liver damage, headache, dizziness, insomnia, fatigue, gastrointestinal discomfort, elevated alanine aminotransferase, musculoskeletal and connective tissue diseases such as creatine phosphokinase, dizziness, general fatigue, indigestion and other symptoms are becoming its side effects to further hinder 3TC efficiency (Dezani *et al*., 2013, Waters *et al*., 2021). More importantly, 3TC belongs to Biopharmaceutics Classification System (BCS) III compound (Dai *et al*., 2015, Sun *et al*., 2023). Due to its high hydrophilicity, it is widely distributed in the extracellular fluid, resulting in reduced liver absorption for the less drug concentration in liver. Naturally, the increased dosage of 3TC will increase its side effects. Meanwhile, the hydrophilic 3TC will limit membrane permeability, thus preparing the lipophilic prodrug becomes one of the main strategies to improve the bioavailability and reduce the side effects (Xiao *et al*., 2019). Furthermore, it may be of great significance to improve the biodistribution characteristics of drugs *in vivo* and improve membrane permeability. As a long-term or even lifelong drug, the obvious side effects will greatly reduce the patient's compliance and even endanger the patient's life.

In order to improve the lipophilicity of hydrophilic drug LA and increase its encapsulation rate and drug loading efficiency in nanocarriers, the long-chain fatty acids were selected as modification groups to carry out the lipophilic modification of LA. Lamivudine palmitate (LAP), derived from the reaction of LA with palmitate, can significantly increase drugs lipid solubility and oil-water partition coefficient, as well as promote the membrane

**Corresponding author:* e-mail: zhuwenquan1984@126.com

permeability of the drug (Singh *et al*., 2017). Ester bond is one of the common chemical ways to prepare prodrugs, which can be hydrolyzed under special physiological environment *in vivo* and then become the original drug (Pandey *et al*., 2020 and Ipar *et al*., 2019). Studies have shown that LAP is relatively stable in a weakly acidic environment and can be hydrolyzed in serum and tissue homogenates, especially be faster hydrolyzed in liver homogenates to achieve LA therapeutic effect. Although the lipid solubility of LAP is increased compared with LA, the direct administration of LAP cannot still effectively improve the biodistribution characteristics of tissues *in vivo* and it fails to avoid hydrolysis before reaching the site of action, thus decreasing the therapeutic effect.

Nanoemulsome (NES) is an emerging drug delivery system that has been widely studied in recent years (Bhuyan *et al*., 2023, Abdulbaqi *et al*., 2021, Li *et al*., 2011). The central nucleus of NES is composed of fat or lipids, and the periphery is surrounded by a phospholipid bilayer. It is a new type of lipid vesicle system with a spherical structure, which has the solid fat nucleus center composed of triglycerides and the phospholipids surroundings, thus exhibiting a good liver-targeting ability. NES has the characteristics of both emulsion and liposome, which can not only encapsulate high concentration of lipophilic drugs in the central hydrophobic nucleus, but also load water-soluble drugs in the phospholipid double-layer water-based compartment. As an excellent carrier for intravenous drug delivery and oral drug delivery, NES has passive targeting of the reticuloendothelial system of the liver and spleen (Chen and Stephen Inbaraj, 2019, Mujugira and Baeten, 2020). In addition, drugs encapsulated in NES can improve their stability by preventing the degradation of drug metabolism enzymes *in vivo*. Meanwhile, NES can be concentrated in the organs rich in macrophages after intravenous injection, thus reduce the accumulation in other organs (Roediger, Smyth and Dieterich, 2022, Scott, 2020). In addition, the slow release of loaded drugs can reduce the local drug concentration to significantly reduce their side effects and the systemic toxic effects.

In this study, to increase the hydrophobicity of LA and improve the *in vivo* membrane permeability of the LA, hexadecanoic acid was linked onto LA to prepare the LAP prodrug. The thin film dispersion method was employed to prepare LAP-NES nanoparticles. The morphology, particle size and Zeta potential of LAP-NES were characterized and the encapsulation drug loading efficiency of LAP-NES was measured. The pharmacokinetics and targeting characteristics of LAP-NES after injection into rat tail vein were investigated, and *in vivo* biodistribution behavior of NES *in vivo* was studied by imaging of small animals. The above results showed that LAP-NES could significantly delay the release of LA *in vivo*, effectively prolong the elimination time and have the characteristics of liver-targeting delivery.

## MATERIALS AND METHODS

### *Materials*

Lamivudine, cetanoic acid, N-(3-Dimethylaminopropyl)-N′-ethylcarbodiimide hydrochloride (EDCI), 4-dimethylaminopyridine, N,N dicyclohexyl carbodiimide, dicyclohexyl carbodiimide, 4-dimethylaminopyridine, Berberine, DiR were purchased from Shanghai Maclin Biochemical Technology Co., LTD. The cholesterol, phospholipids (HSPC) and triglyceride tristearate were provided by A.V.T.n.

### *Methods*

*Synthesis of LAP*

The LA (2.582g), palmitic acid (3.098g), dicyclohexyl carbodiimide (3.000g) and 4-dimethylaminopyridine (0.4128g) were added into a round-bottomed flask and then 200 mL dichloromethane was added with stirring at 25$^{o}$C. After extracting and concentrating to dry by rotary evaporation, the mixed silica gel and dichloromethane were added and mixed evenly. After separating by silica gel column chromatography, the obtained substance was used for spin steaming and structure identification.

### *Synthesis of LAP-NES*

LAP-NES was prepared by the thin film dispersion method. LAP (40mg), cholesterol (300mg), phospholipids (600mg), triglyceride tristearate (40mg) and Tween-80 (600mg) were dissolved evenly with chloroform in a 100mL round-bottomed flask. The organic solvent was evaporated under reduced pressure using a rotary evaporator until a uniform film was formed on the flask wall. Then the 10mL PBS (pH 6.8) was added to hydrate the dry film for 30 min at 40$^{o}$C and the LAP-NES was obtained by ultrasound. The blank NES was prepared without the addition of LAP.

### *Characterizations of LAP-NES*

The appearance of LAP-NES was observed by using a transmission electron microscopy (TEM, Hitach HT-7700, Japan). The particle size, polydispersity index and Zeta potential values of the samples were measured by a nano-size analyzer (Zetasizer Nano-ZS90, Malvern, Worcestershire, UK).

### *Entrapment efficiency and loading efficiency*

The HPLC was used to calculate the loading and entrapment efficiency of LAP-NES. 5mL LAP-NES solution was placed in a 10mL bottle and diluted by PBS (pH 6.8). 2mL LAP-NES dilution was precisely measured, and filtrated by 0.45μm filtration membrane to remove the unencapsulated free drugs and measure the concentration of encapsulated LAP in LAP-NES by HPLC.

Entrapment efficiency (EE%) =(We / Wt)×100%
Loading efficiency (LE%) = (We / Wo)×100%
where We represents the amount of LAP encapsulated in NES, the Wt represents the total amounts of drugs added, the Wo represents the total amounts of the NES.

***In vitro release of the LAP***
The *in vitro* LAP release was determined by dialysis method. Firstly, 2 mL LAP-NES suspension and free LA were placed in a dialysis bag (cut-off size :10000kDa), respectively. And then the dialysis bag was placed in 200 mL release medium (pH=7.4 PBS, containing 0.5% Tween-80) with magnetic stirring at 37±0.5ºC (50r/min). At 0.5, 1, 2, 4, 6, 8, 10, 12, 24, 48 and 72 h, 2 mL solution was removed from the release system and replenished with 2mL blank release medium, and filtrated using 0.45 μm membrane. The sample was analyzed and determined by HPLC, and the cumulative release at each time point was calculated.

***In vivo biodistribution of LAP-NES***
The 24 healthy Kunming (KM) species mice (200-220g) were administrated with free LA (control group) and LAP-NES group, respectively. The free LA group was administrated with free LA (7.2mg/kg) and the LAP-NES group was administrated with LAP-NES sample (equivalent to 7.2mg/kg LA). Each fasted mouse was injected by tail vein with 0.2mL. The mice were sacrificed at 1, 4, 12, 24h after the intravenous injection, and the heart, liver, spleen, lung and kidney tissues were quickly removed and washed with normal saline. The tissue homogenate was obtained from the supernatant of each tissue samples and normal saline solution (weight ratio: volume = 1:3). 100μL internal standard working solution (Berberine hydrochloride) was mixed with 100 μL tissue homogenate evenly and 500μL methanol was added to precipitate protein, the products were collected by centrifugation for detecting the drug content by UPLC-MS/MS.

***Targeting evaluation of tissue biodistribution***
According to the drug concentration data in the tissues, the drug concentration-time curves in the free LA and the LAP-NES were calculated, respectively. The targeted biodistribution characteristics of LAP in mice were evaluated according to peak concentration ratio ($C_e$) and relative uptake rate ($R_e$).

$C_e = (C_{max})e / (C_{max})c$
$(C_{max})e$ represents the LA peak concentration of LAP-NES, $(C_{max})c$ represents the LA peak concentration of free LA group. $C_e>1$ indicates the targeting property of LAP-NES.
$R_e = (AUCi)_e / (AUCi)_c$
Where $(AUCi)_e$ represents Area under the drug-time curve of LAP-NES, $(AUCi)_c$ represents Area under the drug-time curve of free LA. Re>1 indicates the targeting property of LAP-NES, and the targeting effect enhanced with the increase of Re value. Re<1 indicates the non-targeting property of LAP-NES.

***In vivo biodistribution of tissues***
The biodistribution characteristics of NES containing fluorescent dye DiR in mice were investigated by fluorescence imaging *in vivo*. Male KM mice (20±2g) were randomly divided into two groups. Mice were injected intravenously with DiR solution (control group) and DiR-labeled NES at a DiR dose of 2.5 mg/kg. The mice were anesthetized with isoflurane at different time points after administration, respectively. The mice were placed in the camera obscurum of the small animal imager for photography under anesthesia. Fluorescence imaging was obtained at the same exposure intensity and exposure time for photography. After 72 h, their heart, liver, spleen, lung and kidney were taken out and placed in the imager for photography. Fluorescence distribution was compared for investigating the targeted bio-distribution of nanoparticles in mice.

***In vivo pharmacokinetics study***
Twelve male Sprague-Dawley (SD) rats (200-220 g) were randomly divided into two groups for free LA group and LAP-NES group, respectively. The mice were fasted 12 hours before the experiment. The free LA group was given free LA (5mg/kg), and the LAP-NES group was given LAP-NES (equivalent to 5mg/kg free LA) by tail vein. Each rat was intravenous injected with 1mL. At 0.25h, 0.5h, 1h, 1.5h, 2.5h, 4h, 6h, 8h, 10h and 12h after administration, 1 mL blood was taken from the tail vein and the plasma was centrifuged at 4000 r/min. The 100 μL plasma sample was placed in a 1.5 mL centrifugation tube, then 100 μL internal standard solution (50 ng/mL Berberine hydrochloride solution) was added. Then 500 μL methanol was added, vortexed for 2 min, and the supernatant was taken by UPLC-MS/MS analysis.

***Ethical approval***
The Experimental Animal Ethics Committee of Qiqihar Medical College has accepted this research protocol (Report No. QMU-AECC-2021-2228).

## STATISTICAL ANALYSIS

The results were stated as “mean value ± standard deviation” (x ± SD). All analyses were performed using SPSS26.0. A p-value less than 0.05 is considered to indicate a statistically significant difference.

## RESULTS

This section may be divided by subheadings. It should provide a concise and precise description of the experimental results, their interpretation, as well as the experimental conclusions that can be drawn.

**Table 1**: The oil-water partition coefficient of LAP and LA

| Medium | PBS | Water |
|---|---|---|
| LAP | 502 | 381 |
| LA | 0.23 | 0.12 |

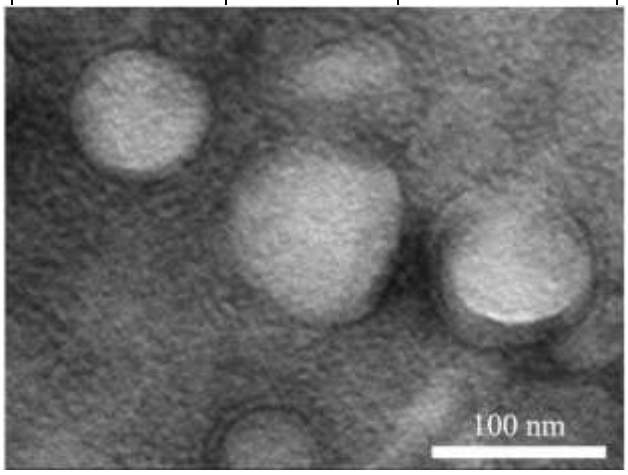


**Fig. 1**: TEM image of LAP-NES (×350000)

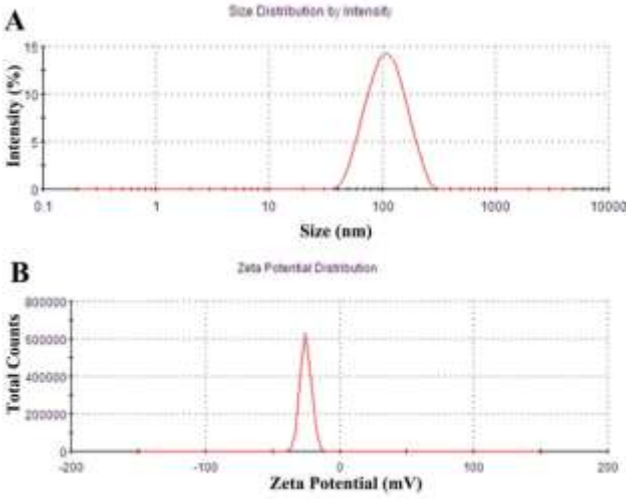


**Fig. 2**: (A) Size distribution of LAP-NES; (B) Zeta potential of LAP-NES

***Determination of oil-water partition coefficient***

The oil-water partition coefficient of prodrugs is crucial for the preparation of NES. Considering that LAP is easily hydrolyzed in alkaline solution and relatively stable in acidic solution, the oil-water partition coefficient of LAP and LA were determined by two aqueous media: deionized water and pH 7.4 PBS. The oil-water partition coefficient of LAP and LA were determined by shaking flask method. And the results are shown in the table 1. The results showed that the oil-water partition coefficients of prod rug LAP in the two media were significantly enhanced compared with that of LA. These results verified the successful synthesis of LAP, which laid the foundation for the subsequent preparation of LAP-NES. Bulleted lists look like this.

***Preparation and the characterizations of LAP-NES***

The LAP-NES was prepared through a lipid film hydration combined with ultrasound and the composition of NES is shown in table 2. As shown in the TEM image in fig. 1, the LAP-NES exhibited spherical vesicles with similar particle size at approximately 100 nm. The particle size and distribution of LAP-NES were measured by Marvin Nano ZS90 Zetasizer particle size analyzer, and the result is shown in fig. 2. The average particle size of LAP-NES was 115.5 nm and the polydispersity index was 0.152. This indicated that the size distribution of the prepared LAP-NES was uniform. The particle size was larger than that observed by TEM because the particle size measured by DLS had hydration layer, while the particle size was measured under dry conditions by TEM. The Zeta potential of LAP-NES was -25.1 mV.

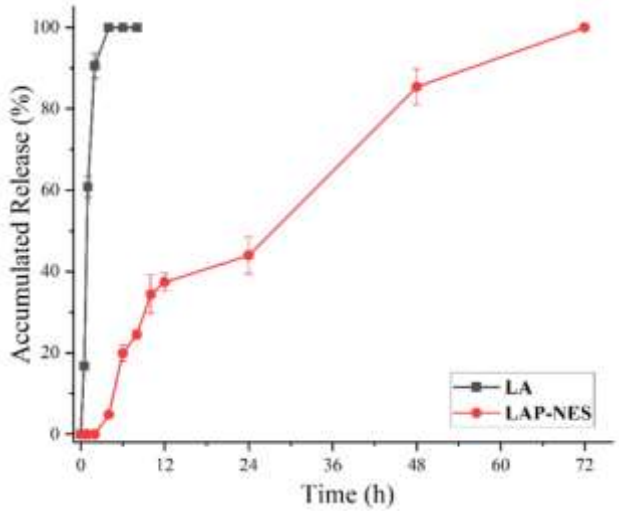


**Fig. 3**: *In vitro* release performances of free LA and LAP-NES in PBS (pH 7.4) containing 0.5% Tween-80

**Table 2**: The composition of NES

| Composition | Dosage |
|---|---|
| LAP | 40 mg |
| cholesterol | 300 mg |
| phospholipid | 600 mg |
| Tristearic acid glycerol ester | 40 mg |
| tween 80 | 600 mg |

**Table 3**: Encapsulation efficiency and loading efficiency of LAP-NES

| Encapsulation efficiency (%) | Loading efficiency (%) |
|---|---|
| 92.30±1.23 | 2.72±0.04 |

The encapsulation and drug loading efficiency of LAP-NES were measured by the HPLC method at 272 nm, as shown in table 3. The encapsulation and drug loading efficiencies of LAP-NES were (92.30±1.23)% and (2.72±0.04)%, respectively. The relative high drug encapsulation efficiency of LAP-NES was due to the good lipid solubility of LAP.

***In vitro release***

*In vitro* drug release performances of LA in LAP-NES were measured by dialysis method in PBS (pH 7.4) containing 0.5% Tween-80. The release results are shown in fig. 3. The free LAP showed the quick release, and the release percentage of LAP was almost 100% at 4h, indicating that the dialysis bag would not affect the release of free drugs. In contrast, LAP-NES showed a slow-release trend. The release of LAP was only 4.8% at 4h and the release rate was up to 85.4% at 48h and reached 100% at 72h. In a word, LAP-NES showed a certain sustained release effect, which was expected to reduce the obvious toxic side effects of drugs.

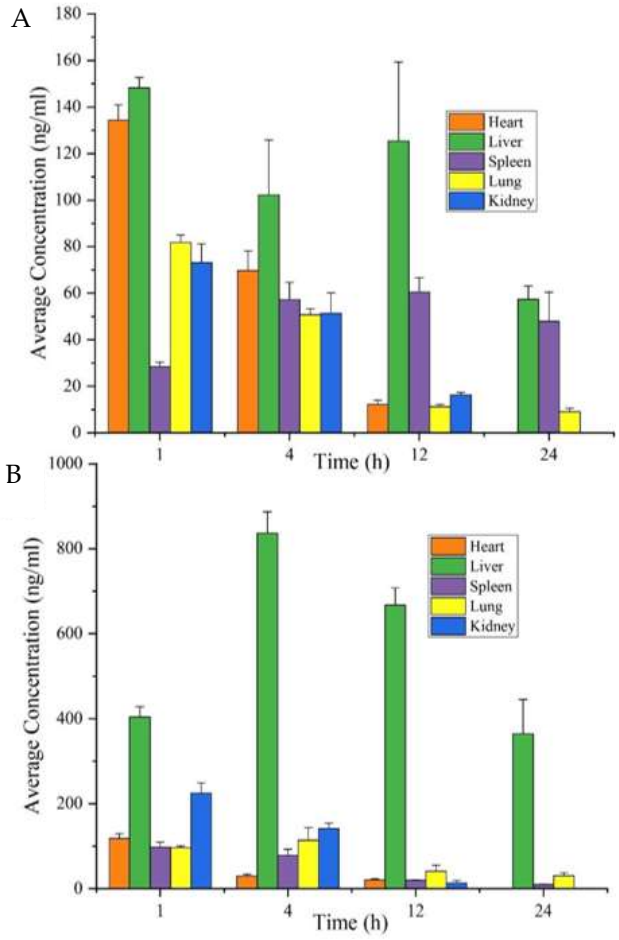


**Fig. 4**: Contents of LA in tissue samples of (A) free LA group and (B) LAP-NES

***In vivo biodistribution of LA***

After intravenous injection in mice at different time intervals, the homogenate concentration data of different tissues in the control group (free LA) and LAP-NES are shown in fig. 5. For the free LA, the concentrations of different tissues in the heart, lung and kidney of the control group reached the highest at 1 h at post-injection, and then the concentration decreased rapidly. The heart concentration was relatively high. In addition, LA content could still be detected in lung tissue at 24h post-injection, while drug concentrations in heart and kidney tissue homogenates could not be quantified. The drug concentration in spleen increased at the first 4 h and then decreased after 12h. The drug concentration in spleen reached the maximum 60.55ng/mL at 12h and 47.93ng/mL at 24h. The concentration of LA in liver was higher than that in other tissues, and the maximum concentration was 148.26ng/mL at 1h post-injection, 125.40ng/mL at 12h post-injection, and 57.38ng/mL at 24 h post-injection.

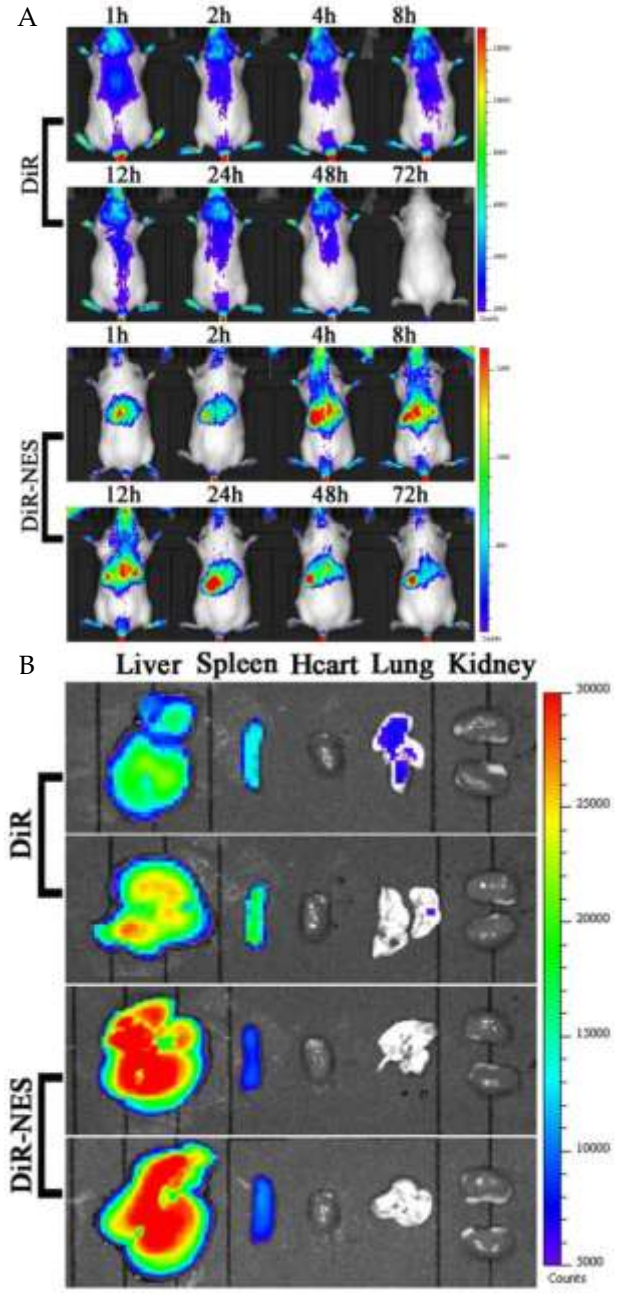


**Fig. 5**: (A) *In vivo* biodistribution of Free DiR and DiR-NES after intravenous injection for 72 h; (B) Ex-vivo biodistribution of Free DiR and DiR-NES after intravenous injection for 72 h.

The concentrations of LA in the heart, spleen and kidney tissues were the highest at 1h after administration, and then the concentration decreased rapidly. The concentrations of LA in the liver and lung gradually increased and then decreased. The peak time of LAP-NES in liver was earlier than that in the control group, at 4h post-injection at highest at 836.97ng/mL, indicating that NES nanoparticles could be distributed to the liver relatively fast after entering the body. The LA concentration in the liver was still 365.16ng/mL at 24h post-injection. Although the concentration of drug in spleen was higher than that in control group in the first 4 h, the concentration decreased rapidly after 24h and the concentration was only 9.99ng/mL.

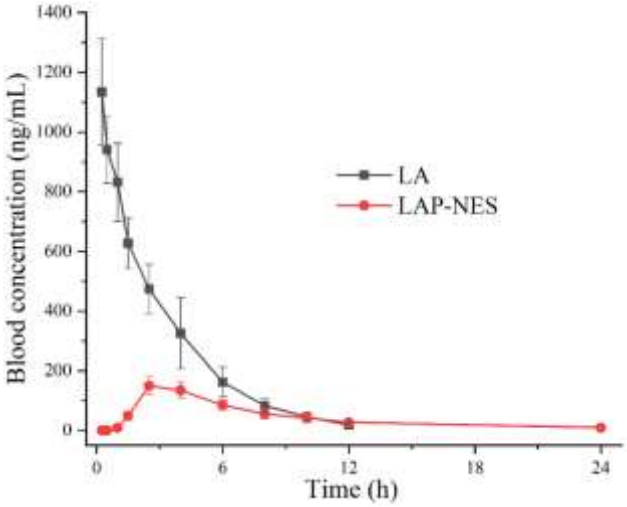


**Fig. 6**: Plasma concentration-time curves of LA

The drug concentrations were calculated in different tissues as shown in fig. 4. As shown in the fig. LA in each tissue of the control group was mainly distributed in the liver both for the free LA group and LAP-NES group. LAP-NES could significantly increase the drug concentration in the liver. The drug concentrations in the liver were about 2.7-fold, 8.2-fold, 5.3-fold, and 6.4-fold compared with that in the free LA group at 1h, 4h 12h and 24h. In addition, the drug concentrations in the spleen, lung and kidney of the LAP-NES group were also higher than that of the free LA group at the first 4h, which was because NES nanoparticles could be quickly recognized by the reticuloendothelial system and were distributed in the above tissues after intravenous injection. However, the drug concentrations in LAP-NES group were lower than that in the free LA group after administration for 12 h, especially the drug concentrations in the LAP-NES group were 0.3 and 0.2 times compared with that in the free LA group after 12h and 24h.

***Targeting evaluation***

Peak concentration ratio (Ce) was calculated according to the peak concentration of LAP-NES and control group (free LA) in different tissues and the relative uptake rate (Re) was calculated by the blood concentration-time curve area of the LAP-NES and control group (free LA) in different tissues as shown in table 4 and table 5. According to the Ce data, LAP-NES could significantly increase the concentration of LA in the liver with the Ce value of 5.65 and the Ce values of each major tissues were Ce (liver) > Ce (kidney) > Ce (spleen) > Ce (lung) > Ce (heart), indicting the good liver-targeting ability of LAP-NES. In addition, LAP-NES could also enhance the targeting of LA in spleen, lung and kidney to varying degrees. According to the Re data, NES could significantly improve the liver-targeting of LA and the liver Re value was 5.81. The Re values in all tissues were Re (liver) >Re (lung) >Re (kidney) >Re (spleen) >Re (heart), further proving that NES had the strongest targeting effect in liver tissue.

***In vivo biodistribution by living imaging***

To study the *in vivo* biodistributions of LAP-NES, a fluorescent probe DiR was encapsulated in LAP-NES to investigate the real-time biodistributions of nanoparticles in different organs after intravenous administration. Mice were injected with DiR solution (control group) and DiR-labeled NES at a dose of 2.5mg/kg DiR by tail vein, respectively. The imaging results of mice *in vivo* at different times are shown in fig. 5A and the ex-vivo tissue imaging images are shown in fig. 5B. As can be seen from the fig. for the free DiR group, DiR was distributed rapidly in the liver, spleen and other tissues without obvious characteristic distribution. The fluorescence intensity was relatively strong at 1 h after administration and gradually decreased and then no obvious fluorescence was observed at 72h.

In contrast, for the DiR-labeled NES, obvious fluorescence distributions were observed in the liver, spleen and other tissues after injection, indicating the good targeting of DiR-labeled NES in the liver and spleen. The fluorescence intensity increased gradually and reached the maximum at 4h and then the DiR fluorescence slowly decreased until 72h. The DiR also showed some biodistribution in the brain. This may be related to the reason that the presence of the lipid inside the NES can improve the ability of drugs to cross the blood-brain barrier. Compared with ex-vivo tissue imaging at 72h the fluorescences in the liver, spleen and lungs of the free DiR group were still present, while the fluorescence intensity in the liver of DiR-NES was stronger than that of the control group.

***Blood concentration-time curves in rats***

The blood drug concentration data of free LA group and LAP-NES at different time points after injection through the tail vein were calculated. The blood drug concentration-time curves of LA are shown in fig. 6. According to the data, for free LA group, the blood concentration reached the highest at 0.25h after

administration and the average blood concentration reached 1134.28ng/mL. After that, the concentration decreased rapidly to 17.95ng/mL at 12h.

The plasma concentration of LA was lower than the limit of quantitation after 24 h, proving that the drug was basically eliminated. For LAP-NES group, the blood drug concentration of LAP could not be detected after administration. In contrast, the LA could be detected within 1h. The blood concentration of LA increased first and then decreased. The LA concentration reached the highest at 2.5h after administration with an average concentration of 149.60ngmL and then decreased slowly to 27.26ng/mL at 12 h and 9.08ng /mL at 24h. This may be because the prodrug LAP loaded in LAP-NES was gradually released into the blood slowly after intravenous injection, and the released LAP was further hydrolyzed into prototype drug LA by a large number of non-specific hydrolytic enzymes *in vivo*. Hence, the content of LAP was very low and did not reach the limit of quantification. The LAP-NES could slowly and continuously release LAP into the blood, resulting in a low concentration of LA before 1h which was below the quantitation limit. And the LA concentration could be quantified after 1h. Therefore, the elimination rate of LA in the blood for LAP-NES group was lower compared with the free LA group, which was ascribed to the slowed release of LAP in LAP-NES.

The pharmacokinetic parameters of LA were obtained using pharmacokinetic processing software DAS 2.0 and non-atrioventricular model, as shown in table 6. According to the data, for free LA, the blood concentration reached the maximum promptly after administration, with the tmax of 0.25 h, $t_{1/2}$ of 2.12h, AUC of 3501.74μg/L·h and MRT of 2.95h. For the LAP-NES group, the peak time was delayed and tmax was 2.5h. The $t_{1/2}$ (4.09 h) was about 1.9 times compared with the solution group, which may be related to the slowed release of LAP in LAP-NES. The mean retention time was extended with the MRT of 8.13h, indicating that LAP-NES had a good slow-release effect. In addition, the AUC was lower than that in the free LA. *In vivo* pharmacokinetic studies showed that the plasma concentration of LA in LAP-NES group was significantly lower than that of the control group, which might be explained by the fact that LAP-NES nanoparticles were quickly uptaken by the reticuloendothelial system and entered the liver and spleen after injected into blood, leading the very low LA concentration in the blood. This was consistent with the results of *in vivo* biodistribution. These results suggested that NES nanoparticles can target the liver and spleen *in vivo* and reduce the drug toxicity.

## DISCUSSION

Lamivudine hexadecylate ester, as a precursor drug of lamivudine, can be rapidly metabolized and hydrolyzed into the original drug lamivudine by non-specific esterases in the body after entering the body (Dezani *et al*., 2013). After administration of lamivudine hexadecylate emulsion through the tail vein of rats, no precursor drugs were detected in the plasma, or the content was too low to be quantified, but the original drug lamivudine could be detected, and the blood concentration could reach the limit of quantification within 24 hours (Chen *et al*., 2019). After administration, the blood drug concentration in the liposome group showed a trend of first increasing and then decreasing, and $C_{max}$ was lower than that in the solution group. This may be due to the slow release of drugs in the liposome. After being injected into the blood through the tail vein of rats, lactosomes are quickly absorbed by the reticuloendothelial system and distributed to the liver, spleen, and other parts, resulting in a low content of lactosomes in the blood and a low amount of metabolized drugs after drug release, resulting in a lower concentration of drugs in the lactosomes group than in the solution group. As the distribution process progresses, drugs distributed in the tissue are slowly released from the lactose, metabolized into prototype drugs and enter the bloodstream, causing the concentration of drugs in the blood to begin to increase (Sun *et al*., 2023). At the same time, as the drug in the tissue continues to slowly release and distribute, the drug is continuously distributed from the tissue into the blood to supplement the elimination of drug concentration in the blood. Therefore, the blood drug concentration first increases and then slowly decreases. And this result is basically consistent with the in vivo imaging results of mice.

In the determination of the drug content *in vivo* biodistribution, for the LAP-NES group, the prodrug LAP could not be detected in other tissues except the liver tissue after administration, but the concentration of LAP in the liver was still too low and could not be quantified. Hence, it could be speculated that the prodrug LAP could be rapidly metabolized into the original drug LA after the LAP was released form LAP-NES *in vivo*, so that the LAP concentration became too low to be detected. In contrast, the contents of LA could be measured in the homogenate samples at all time points. The concentrations of drug in the samples of liver, spleen, lung and kidney tissues of LAP-NES group were higher than that of the control group except for the heart.

DiR solution (dye control group) and DiR labeled liposomes (administration group) were administered to mice through tail vein injection at a dose of 2.5 mg/kg, respectively. The stronger the fluorescence intensity, the more fluorescent dyes accumulated in this area (Xiao *et al*., 2019). The imaging results of mice at different times showed that DiR was rapidly distributed in the body after administration in the fluorescent dye group, although it was distributed in liver, spleen and other parts, but there

was no obvious characteristic distribution. After 1 hour of administration, the fluorescence intensity was strong, and then gradually decreased. After 72 hours, there was no obvious fluorescence. After injection, the lactosome administration group began to produce a significant distribution in the liver, spleen and other parts, reflecting the characteristic of lactosomes targeting the liver and spleen. And the fluorescence intensity showed a trend of first increasing and then decreasing, with the highest fluorescence intensity at 4 hours and then slowly weakening, and still having fluorescence intensity at 72 hours. It appears to have a certain distribution outside the brain. This may be related to the fact that the presence of the lipid core of the liposome can enhance the ability of drugs to penetrate the blood-brain barrier. In the in vivo biological distribution of in vivo imaging, compared to 72 hour in vitro tissue imaging, fluorescence still exists in the liver, spleen, and lungs of the free DiR group. However, the fluorescence intensity of DiR-NES in the liver was stronger than that of the control group, indicating the accumulation of nanoparticles in the liver and spleen, which is consistent with in vivo imaging results. This may be due to the fact that NES can be absorbed by the monocyte macrophage system after intravenous injection, exhibiting obvious liver spleen targeting characteristics (Ipar *et al*., 2019). In addition, compared with the control group, the lung fluorescence in the DiR-NES group significantly disappeared 72 hours later, indicating that NES can reduce the distribution of drugs in other tissues, improve liver targeting characteristics, and thus reduce toxic side effects.

## CONCLUSIONS

LA was made into prodrug LAP and encapsulated in NES to increase its poor lipid solubility and reduce the obvious toxicity. The LAP-NES was prepared by the film dispersion method and the average encapsulation efficiency of LAP was 92.30%. The prepared LAP-NES was shape-like intact round vesicles with an average particle size of 115.5nm, PDI value of 0.152 and Zeta potential of -25.1 mV. The *in vivo* biodistributions of LAP-NES in liver, lung, kidney and other tissues were significantly improved after injection into the tail vein of mice with the highest distribution in the liver, indicating the excellent liver-targeting ability of LAP-NES. The plasma concentration of LAP-NES increased at the 2.5h and then decreased slowly after injection into the tail vein of rats, and the biological half-life, clearance rate and average retention time of LAP-NES prolonged compared with free LAP. The *in vivo* biodistribution results showed that LAP-NES could improve the liver biodistribution of drugs, thus showing the liver-targeting characteristics. In summary, LAP-NES shows excellent fluorescence localization performance and great potential for liver-targeting delivery to increase the therapeutic effect and decrease the side effects of LA.

## ACKNOWLEDGMENTS

This research was funded by Heilongjiang Provincial Department of Education Science and Technology Research Project, grant number 2018-KYYWF-0096.

## REFERENCES

Abdulbaqi IM, Assi RA, Yaghmur A, Darwis Y, Mohtar N, Parumasivam T, Saqallah FG and Wahab HA (2021). Pulmonary delivery of anticancer drugs via lipid-based nanocarriers for the treatment of lung cancer: An Update. *Pharmaceuticals-Base,* **14**(8): 725-763.

Belopolskaya M, Avrutin V, Kalinina O, Dmitriev A and Gusev D (2021). Chronic hepatitis B in pregnant women: Current trends and approaches. *World J. Gastroentero*, **27**(23): 3279-3289.

Bhuyan M, Kaur M, Kaushal U, Nagpal M, Singh M, Aggarwal G (2023). Recent avenues in treatment of liver diseases: Role of nanotechnology. *Curr. Drug Targets,* **24**(4): 320-331.

Chen BH and Stephen Inbaraj B (2019). Nanoemulsion and nanoliposome based strategies for improving anthocyanin stability and bioavailability. *Nutrients,* **11**(5): 1052-1072.

Choi YM, Kim H, Lee SA, Lee SY and Kim BJ (2020). A telomerase-derived peptide exerts an anti-hepatitis b virus effect via mitochondrial dna stress-dependent type i interferon production. *Front Immunol.*, **11**: 652.

Chow N, Wong D, Lai CL, Mak LY, Fung J, Ma HT, Lei MW, Seto WK and Yuen MF (2023). Effect of Antiviral Treatment on Hepatitis B Virus Integration and Hepatocyte Clonal Expansion. *Clin. Infect. Dis.*, **76**(3): 801-809.

Dai JJ, Tao HM, Min QX and Zhu QH (2015). Anti-hepatitis B virus activities of friedelolactones from Viola diffusa Ging. *Phytomedicine,* **22**(7-8): 724-729.

Dezani AB, Pereira TM, Caffaro AM, Reis JM, Serra CH (2013). Determination of lamivudine and zidovudine permeability using a different ex vivo method in Franz cells. *J. Pharmacol. Tox. Met.*, **67**(3): 194-202.

Guo PL, He HL, Chen XJ, Chen JF, Chen XT, Lan Y, Wang J, Du PS, Zhong HL, Li H, Liu C, Li LY, Hu FY, Tang XP, Cai WP and Li LH (2020). Antiretroviral long-term efficacy and resistance of lopinavir/ritonavir plus lamivudine in HIV-1-infected treatment-naive patients (ALTERLL): 144-week results of a randomized, open-label, non-inferiority study from Guangdong, China. *Front. Pharmacol.*, **11**: 569766.

Ipar VS, Dsouza A and Devarajan PV (2019). Enhancing curcumin oral bioavailability through nano-formulations. *Eur. J. Drug Metab. Ph.*, **44**(4): 459-480.

Li H, Xiao Y, Niu J, Chen X and Ping Q (2011). Preparation of a cationic nanoemulsome for

intratumoral drug delivery and its enhancing effect on cellular uptake *in vitro*. *J. Nanosci. Nanotechno*, **11**(10): 8547-55.

Martinez de Lagran M, Elizalde-Torrent A, Paredes R, Clotet B and Dierssen M (2022). Lamivudine, a reverse transcriptase inhibitor, rescues cognitive deficits in a mouse model of down syndrome. *J. Cell Mol. Med.*, **26**(15): 4210-4215.

Mujugira A, Baeten JM, Hodges-Mameletzis I and Haberer JE (2020). Lamivudine/tenofovir disoproxil fumarate is an appropriate PrEP regimen. *Drugs*, **80**(18): 1881-1888.

Pandey P, Gulati N, Makhija M, Purohit D and Dureja H (2020). Nanoemulsion: A novel drug delivery approach for enhancement of bioavailability. *Recent Pat Nanotech*, **14**(4): 276-293.

Roediger R, Smyth EK and Dieterich D (2022). Adefovir for lamivudine-resistant hepatitis B. *Antivir Ther*, **27**(2): 1-8.

Scott LJ (2020). Dolutegravir/lamivudine single-tablet regimen: A review in HIV-1 infection. *Drugs*, **80**(1): 61-72.

Singh Y, Meher JG, Raval K, Khan FA, Chaurasia M, Jain NK and Chourasia MK (2017). Nanoemulsion: Concepts, development and applications in drug delivery. *J. Control Release*, **252**: 28-49.

Stinco M, Rubino C, Trapani S and Indolfi G (2021). Treatment of hepatitis B virus infection in children and adolescents. *World J. Gastroentero.*, **27**(36): 6053-6063.

Sun Y, Wang S, Li Y, Wang D, Zhang Y, Zhang H, Lei H, Liu X, Sun J, Sun B and He Z (2023). Precise engineering of disulfide bond-bridged prodrug nanoassemblies to balance antitumor efficacy and safety. *Acta Biomater.*, **157**: 417-427.

Waters L, Mehta V, Gogtay J and Boffito M (2021). The evidence for using tenofovir disoproxil fumarate plus lamivudine as a nucleoside analogue backbone for the treatment of HIV. *J. Virus Erad.*, **7**(1): 100028.

Xiao C, Hu H, Yang H, Li S, Zhou H, Ruan J, Zhu Y, Yang X and Li Z (2019). Colloidal hydroxyethyl starch for tumor-targeted platinum delivery. *Nanoscale Adv*, **1**(3): 1002-1012.